Journal Name

ARTICLE

Two-dimensional CaSi monolayer with quasi-planar pentacoordinate silicon†

Received 00th January 20xx,
Accepted 00th January 20xx

DOI: 10.1039/x0xx00000x

www.rsc.org/

Yu Wang,[a] Man Qiao,[a] Yafei Li*[a] and Zhongfang Chen*[b]

The prediction of new materials with peculiar topological properties is always desirable to achieve new properties and applications. In this work, by means of density functional theory computations, we extend the rule-breaking chemical bonding of planar pentacoordinate silicon (ppSi) into the periodic system: a C_{2v} $Ca_4Si_2^{2-}$ molecular building block containing a ppSi center is identified firstly, followed by the construction of infinite CaSi monolayer, which is essentially a two-dimensional (2D) network of the Ca_4Si_2 motif. The moderate cohesive energy, absence of imaginary phonon modes, and good resistance to high temperature indicate that CaSi monolayer is a thermodynamically and kinetically stable structure. Especially, a global minimum search reveals that the ppSi-containing CaSi monolayer is the lowest-energy structure in 2D space, indicating its great promise for experimental realization. CaSi monolayer is a natural semiconductor with an indirect band gap of 0.5 eV, and it has rather strong optical absorption in the visible region of solar spectrum. More interestingly, the unique atomic configuration endows CaSi monolayer an unusual negative Poisson's ratio. The rule-breaking geometric structure together with its exceptional properties makes CaSi monolayer a quite promising candidate for electronics, optoelectronics, and mechanics applications

Conceptual insights

Chemical bonding is one of the most basic concepts of chemistry, and many established bonding rules are the foundations for the understanding of structure and electronic properties of molecules and solids. Therefore, designing new materials with rule-breaking chemical bonding, e. g. planar hypercoordinate motifs, would be of both theoretical and practical importance. Based on multi-scale simulations, we demonstrate that two-dimensional CaSi monolayer, in which each Si atom binds with five ligands to form a moiety of quasi-planar pentacoordinate silicon, is thermodynamically, dynamically and thermally stable. Our designed CaSi monolayer is the global minimum structure in 2D space; it possesses a moderate band gap and exhibits unusual negative Poisson's ratios.

Introduction

Most main-group elements obey some established rules when forming chemical bonds with other elements and themselves. For example, the tetrahedral preference of saturated sp^3 carbon (C) in most known molecules and materials has been established as one of the foundations of organic chemistry.[1,2] In addition, C also has a vast flexibility to adopt the linear *sp* or planar sp^2 hybridization coupled with the right valence. In 1968 Monkhorst proposed the rule-breaking "planar tetracoordinate carbon" (ptC) by exampling the fictitious planar methane (D_{4h}),[3] which is actually not a local minimum structure. Hoffmann *et al.*[4] then suggested that the ptC moiety can be stabilized electronically by using π-acceptor or σ-donor ligands, or mechanically by enforcing ptC arrangements in strained rings or cages. Under this guidance, Collins *et al.*[5] designed the first ptC-containing molecule (1,1-dilithiocyclopropane) by *ab initio* computations. In 1977, the first experimentally verified ptC molecule was achieved by Cotton and co-workers.[6] In 1991, Boldyrev and Schleyer proposed the bonding rules on the basis of electronic and geometrical considerations to guide the design of ptC-containing molecules,[7] which significantly promotes the development of planar carbon chemistry.[8-11] Encouragingly, some global minimum ptC species, such as CAl_4^-,[12] CAl_4^{2-},[13] CAl_3Si^-,[14] and their derivatives have been identified experimentally by gas-phase photoelectron spectroscopy. More excitingly, the existence of planar hypercoordinate carbons with coordination number larger than four, such as planar pentacoordinate carbon (ppC)[15,16] and hexacoordinate carbon (phC)[17,18] have also been explored theoretically. These fantastic new bonding arrangements are of

[a] Jiangsu Collaborative Innovation Centre of Biomedical Functional Materials, Jiangsu Key Laboratory of New Power Batteries, School of Chemistry and Materials Science, Nanjing Normal University, Nanjing 210023, China. Email: liyafei@njnu.edu.cn
[b] Department of Chemistry, Institute for Functional Nanomaterials, University of Puerto Rico, Rio Piedras Campus, San Juan, PR 00931, USA. Email: zhongfangchen@gmail.com

† Electronic Supplementary Information (ESI) available. See DOI: 10.1039/x0xx00000x

fundamental significance and have important implications in designing new materials.

As another group-14 element, silicon (Si) has distinct bonding characters from those of carbon. For instance, Si tends to utilize all three of its 3*p* orbitals to adopt the tetrahedral sp^3 hybridization whereas the planar hybridization of silicon is rather rare in nature. The extensive studies of planar hypercoordinate carbon have also motivated scientists to explore molecules with planar hypercoordinate silicon, especially considering that the planar tetracoordination is fundamentally easier to realize with silicon than with carbon.[19] In 1979 Schleyer *et al.* predicted theoretically the first molecule containing a planar tetracoordinate silicon (ptSi) center, i. e. orthosilicic acid ester.[20] Afterwards, many ptSi-containing molecules were designed computationally, such as tetraazafenestrane,[21] and $Si(CO)_4$.[22] However, none of these molecules have been realized experimentally. The breakthrough occurred in 2000, Boldyrev *et al.*[23] detected the first ptSi-containing molecule $SiAl_4^-$ by a joint experimental and theoretical study. In 2004, Li *et al.*[24] proposed a scheme to incorporate ptSi, planar pentacoodinate silicon (ppSi) and hexacoordinate silicon (phSi) in C_{2v}-B_nE_2Si (E = CH, BH, or Si; n = 2-5). Islas *et al.*[25] designed several planar hypercoordinate silicon species by enclosing Si atom in boron wheels. These studies significantly enriched the family of planar hyercoordinate silicon moieties. However, at present there are few studies focusing on planar hypercoordinate silicon and the global minimum structures with planar hypercoordinate silicon are rather rare.

It is known that the properties of a material are mainly determined by its structure, and the unique geometric structures usually lead to exotic physicochemical properties. Therefore, it is desirable to extend the bonding arrangements of planar hypercoordinate carbon and silicon into periodic solids and nanostructures, which would bring some unique structures as well as peculiar potentials for wide applications. The past decade has witnessed the rapid development of this field.[26-28] Especially, stimulated by the isolation of graphene and two dimensional (2D) inorganic materials, there have been growing interests in the design of 2D materials containing planar hypercoordinate carbon or silicon, e. g. ptC-containing B_2C,[29] TiC,[30] and Al_2C monolayers,[31,32] ppC-containing Be_5C_2 monolayer,[33] phC-containing Be_2C monolayer,[34] and ptSi-containing SiC_2 monolayer.[35] The novel geometric structures endow these 2D materials with many intriguing properties. For example, Wang *et al.*[33] demonstrated that Be_5C_2 monolayer is semimetallic and has an unusual negative Poisson's ratio in the in-plane direction, thus is appealing for specific applications in electronics and mechanics. The 2D Cu_2Si monolayer with phSi bonding was theoretically predicted by Yang *et al.* in 2015,[36] and was just synthesized by Feng *et al.*[37] Besides the unique bonding, Cu_2Si presents intriguing Dirac nodal line fermions which open new avenues to realize high-speed low-dissipation devices.[37] Nevertheless, to the best of our knowledge, there is no attempt on designing nanostructures with ppSi, which may be due to the difficulty in finding a suitable type of ligand to electronically or mechanically fit the ppSi in periodic systems.

Here, inspired by the bonding pattern of our newly discovered ppSi species $Ca_4Si_2^{2-}$, we recognize that calcium (Ca) is a promising ligand to construct the ppSi-containing solids. Along this line, we computationally designed a new ppSi-featured 2D material, namely CaSi monolayer, in which each Si atom binds with four Ca atoms and one Si atom in almost the same plane to form a quasi ppSi moiety. The ppSi-containing CaSi monolayer has good thermodynamic, kinetic, and mechanical stabilities and is the global minimum structure in 2D space. Due to the exotic geometric structure, CaSi monolayer presents rather attractive electronic, optical, and mechanical properties.

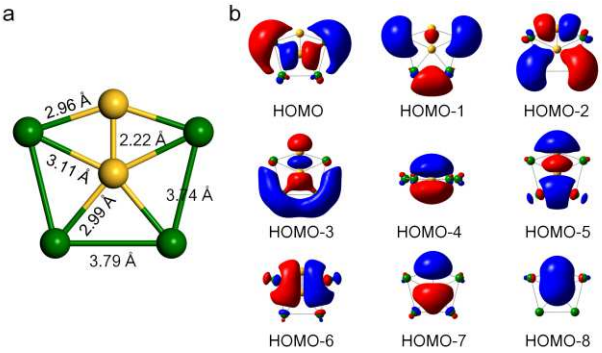

Fig. 1 (a) Optimized atomic configuration of $Ca_4Si_2^{2-}$ molecule computed at M06-2X/cc-pVTZ level. The yellow and green balls represent Si and Ca atoms, respectively. (b) The canonical molecular orbitals of $Ca_4Si_2^{2-}$.

Methods

For $Ca_4Si_2^{2-}$, the geometry optimizations and electronic structure computations were performed at the M06-2X[38] level of theory with the cc-PVTZ basis set as implemented in Gaussian 03 package.[39] The M06-2X functional has been demonstrated to be rather satisfactory for systems consisting of main group elements. The validity of the M06-2X functional for $Ca_4Si_2^{2-}$ cluster and the PBE functional used for slab model computations was verified by comparison with the CCSD(T)[40] and other common methods for the $Ca_4Si_2^{2-}$ cluster (Table S1, ESI†). For CaSi monolayer, DFT computations were performed using Vienna ab initio simulation package (VASP),[41] with exchange-correlation interactions modeled by Perdew–Burke–Ernzerhof functional.[42] Ion-electron interaction was described using the projector-augmented plane wave (PAW) approach.[43,44] The Brillouin zone was sampled with 6×8×1 *k*-points. The convergence threshold was set as 10^{-5} eV in energy and 10^{-2} eV/Å in force. The HSE06 hybrid functional[45] was adopted for high-accuracy electronic structure computations. The phonon spectrum was computed using the finite displacement method as implemented in Phonopy code.[46]

The bonding pattern of CaSi monolayer was analyzed utilizing the Solid State Adaptive Natural Density Partitioning (SSAdNDP) method,[47] which is an extension of the AdNDP method to periodic systems and as such was derived from periodic implementation of the Natural Bond Orbital (NBO) analysis. SSAdNDP allows the interpretation of chemical bonding with translational in terms of classical lone pairs and two-center bonds, as well as multi-center delocalized bonds.

The thermal stability of CaSi monolayer was assessed by utilizing first principles molecular dynamic (FPMD) simulations within PBE

functional as implemented in VASP. The initial configuration with 3 × 4 supercell was annealed at the three temperatures. Each FPMD simulation (NVT ensemble) lasted for 10 ps with a time step of 1.0 fs. Temperature control is fulfilled using Nosé-Hoover method.[48]

The global minimum search for the lowest-energy structure of 2D CaSi was conducted using the particle-swarm optimization (PSO) method within the evolutionary scheme as implemented in the CALYPSO code.[49] The population size as well as the number of generations was set to be 30 in all PSO simulations. We did three structural searches with the unit cell of CaSi monolayer containing 4, 8, and 16 atoms, respectively. The structure relaxations during the PSO simulation were performed using the PBE functional as implemented in VASP. All the obtained structures from CALYPSO search were re-optimized using VASP.

Results and discussion

$Ca_4Si_2^{2-}$: an inspiring ppSi specie for 2D system

Our design of 2D infinite ppSi-containing system was initially motivated by the discovery of ppSi-containing $Ca_4Si_2^{2-}$ minimum (Fig. 1a), which has the singlet ground state with the lowest vibrational frequency being 34.2 cm^{-1} at the M06-2X/cc-pVTZ level of theory. $Ca_4Si_2^{2-}$ has totally 18 valence electrons. As suggested by Boldyrev *et al.*,[8,14] the 17- and 18-electron systems are most promising to form planar configurations. In $Ca_4Si_2^{2-}$, the center Si atom binds with four peripheral Ca atoms and one peripheral Si atom in the same plane, resulting in the formation of ppSi species with C_{2V} symmetry. To our best knowledge, $Ca_4Si_2^{2-}$ is the first hexatomic species containing a ppSi center. The bond lengths between ppSi atom and Ca atoms are 2.99 and 3.11 Å, respectively, while the Ca−Ca bond lengths are 3.74 and 3.79 Å, respectively. Especially, the Si−Si bond length (2.22 Å) is shorter than that of disilane (2.36 Å) but close to that of disilene (2.15 Å), implying its partial double bond feature.

The natural population analysis (NPA) charges and the Wiberg bond index (WBI) were then computed at the M06-2X/cc-pVTZ level of theory to understand the bonding characteristics of $Ca_4Si_2^{2-}$. According to our computations, the ppSi atom is negatively charged (NPA charge -1.55) and the natural electron configuration is $3s^{1.52}3p_x^{1.05}3p_y^{1.60}3p_z^{1.34}$. These results suggest that ppSi in $Ca_4Si_2^{2-}$ is mainly stabilized by the σ-donation of Ca atoms and the delocalization of silicon $3p_z$ electrons. The WBI for ppSi−Ca bonds are 0.29 and 0.30, respectively, while the WBI of Si−Si bond is 1.90, resulting in a total WBI of 3.08 for the center ppSi.

To further understand how the ppSi is stabilized in $Ca_4Si_2^{2-}$, we scrutinized the canonical molecular orbitals of $Ca_4Si_2^{2-}$. As shown in Fig. 1b, most occupied molecular orbitals correspond to the σ bonding of ppSi as well as those between the peripheral Ca and Si atoms. Especially, the HOMO-3 is a highly delocalized π orbital and the HOMO-4 is a delocalized σ orbital, which could intrinsically help maintain the planar configuration. Interestingly, the number of π electrons in $Ca_4Si_2^{2-}$ satisfies the Hückel (4n+2) π-electron rule (n = 0), revealing the aromaticity of $Ca_4Si_2^{2-}$. Moreover, the considerable HOMO−LUMO gap

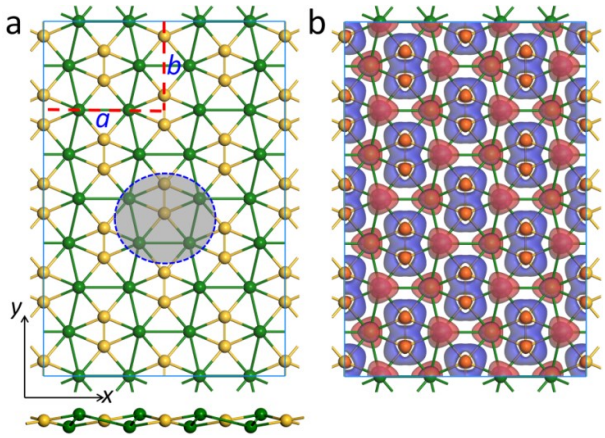

Fig. 2 (a) Top (upper) and side (bottom) views of optimized geometric structure of CaSi monolayer. The red dashed lines label a unit cell, *a* and *b* represent the lattice vectors. The blue dashed circle denotes a Ca_4Si_2 motif. (b) Deformation electron density of CaSi monolayer computed using PBE functional. Blue and red represent electron accumulation and depletion regions, respectively.

(2.12 eV) also suggests the high stability of $Ca_4Si_2^{2-}$. Interestingly, $Ca_4Si_2^{2-}$ anion can be neutralized by two protons (H^+) to form a neutral molecule of $Ca_4Si_2H_2$, which is a local minimum with the lowest vibrational frequency of 26.4 cm^{-1}. In contrast to $Ca_4Si_2^{2-}$, $Ca_4Si_2H_2$ has a slightly buckled rather than planar configuration (Fig. S1, ESI†)

Geometric structure of CaSi monolayer.

Inspired by the bonding pattern of ppSi-containing $Ca_4Si_2^{2-}$, we designed a new ppSi featured 2D material, namely CaSi monolayer. As shown in Fig. 2a, the unit cell of CaSi monolayer consists of four Si atoms and four Ca atoms in a rectangular shape, with the lattice parameters of a and b being 9.33 and 6.86 Å, respectively optimized using PBE functional (a = 9.39 Å and b = 6.91 Å by HSE06 functional). In CaSi monolayer, each Si atom binds with one Si atom and four Ca atoms nearly in the same plane, forming a quasi ppSi moiety akin to $Ca_4Si_2^{2-}$. Interestingly, in CaSi monolayer, each ppSi atom also severs as a ligand of its neighboring ppSi atom. Therefore, CaSi monolayer can be regarded as a result of embedding Si−Si dimers into the distorted Ca hexagonal lattice.

Similar to our previously designed phC-containing Be_2C monolayer[34] and ppC-containing Be_5C_2 monolayer,[33] CaSi monolayer is not purely planar. As can be seen from the side view (Fig. 2a), Ca atoms of CaSi monolayer are buckled into two different atomic layers, which are 0.38 Å above or below the Si atomic layer, respectively. The total degrees of three Ca-Si-Ca angles and two Ca-Si-Si angles associated with one ppSi is 364.44°, which is quite close to the ideal 360°, indicating the good planarity of ppSi moieties in 2D CaSi monolayer. The lengths of Si−Ca (2.97 Å, 3.04 Å) and Si−Si bonds (2.27 Å) of CaSi monolayer are quite close to those of $Ca_4Si_2^{2-}$, whereas the Ca−Ca bond lengths (3.61 Å, 3.98 Å) depart a little from those of $Ca_4Si_2^{2-}$. Interestingly, CaSi monolayer can be entirely planar by applying a biaxial tensile strain of 3.4%. However,

this purely planar structure is 16 meV/atom higher in energy than the buckled one. According to the Hirshefeld charge population analysis, in CaSi monolayer, Si and Ca atoms possess −0.25 |e| and 0.25 |e| charge, respectively. The out-of-plane buckling in the CaSi monolayer could minimize the repulsive interactions between Ca cations as well as maintain the intensity of in-plane Si−Ca and Si−Si bonds, which is favorable for the stabilization of the whole structure.

To understand the unique chemical bonding and the stabilizing mechanism of ppSi moieties in 2D CaSi monolayer, we first plotted its deformation electronic density, which is defined as the difference between the total electronic density and the electronic density of the isolated Si and Ca atoms. Significant electron transfer occurs from the 4s orbital of Ca atoms to Si atoms (Fig. 2b), which are delocalized over the Si−Si and Ca−Si bonds, contributing to the stabilization of ppSi moieties. Moreover, some electrons are also extracted from the $3p_z$ of Si atoms to further stabilize the ppSi moieties. Similar stabilization mechanism has also been revealed in other 2D nanomaterials with planar hypercoordinate motiey.[29-37]

To give a more robust analysis of chemical bonding and to understand in more detail how the lattice bonds of CaSi monolayer are formed, we further employed the recently developed SSAdNDP method to analyze the CaSi monolayer. According to the SSAdNDP analysis (Fig. S2, ESI†), one unit cell of CaSi monolayer contains two 2c-2e Si−Si bonds, eight 3c-2e σ bonds on eight Ca−Si−Ca triangles, and two 4c-2e π bonds on two Ca−Si−Ca−Si rhombuses, accounting for 24 valence electrons per unit cell. Noteworthy, the two Si atoms and two Ca atoms involved in a 4c-2e π bond are exactly in the same plane. The deduced bonding picture is consistent with the symmetry of 2D network. Therefore, it is the existence of multicenter delocalized σ and π bonds that help maintain the quasi planar configuration of CaSi monolayer.

Stability

Although CaSi monolayer has quite charming topological properties and some intrinsic stabilization factors, physically whether it is a stable structure is still pending. To address this issue, we first computed the cohesive energy of CaSi monolayer, which is defined as: $E_{coh} = (nE_{Si}+nE_{Ca}-E_{CaSi})/2n$, in which E_{Si}, E_{Ca} and E_{CaSi} are the total energies of a single Si atom, a single Ca atom, and CaSi monolayer, respectively, and n is the number of Si/Ca atoms in the supercell. Physically, the cohesive energy is a reasonable descriptor for the binding strength of connected frameworks. Though smaller than that of the CaSi Zintl phase (3.77 eV/atom), the cohesive energy of CaSi monolayer (3.07 eV/atom) is comparable to those of the experimentally realized 2D silicene (3.91 eV/atom),[50] germanene (3.24 eV/atom),[51] and stanene (2.73 eV/atom)[52] computed at the same theoretical levels, indicating the strongly bonded CaSi monolayer.

The kinetic stability of CaSi monolayer can be confirmed by the phonon curves where no appreciable imaginary phonon mode is observed (Fig. 3). Remarkably, the highest frequency of CaSi monolayer (475 cm^{-1}) is even higher than those in MoS_2 monolayer (473 cm^{-1})[53] and Cu_2Si monolayer (420 cm^{-1}),[36] but lower than that of silicene (550 cm^{-1}).[54] According to the analysis of the phonon density of states, the highest frequency modes of CaSi monolayer mainly correspond to the Si−Si bonds. Note that the purely planar CaSi monolayer achieved by a biaxial tensile strain of 3.4% is also dynamically stable as all phonon branches are positive in the entire Brillouin zone (Fig. S3, ESI†).

Moreover, we also performed first-principles molecular dynamic (FPMD) simulations to evaluate the thermal stability of CaSi monolayer. Three independent FPMD simulations (900, 1200, and 1500K) were carried out using a 3 × 4 supercell. As shown in Fig. S4, ESI†, CaSi monolayer can keep its structural integrity with slight out-of-plane distortions throughout a 10 ps FPMD simulation up to 1200 K, suggesting that the ppSi-featuring 2D CaSi phase can be separated by an enough barrier from other minimum structures on the potential energy surface, indicative of good thermal stability. In addition, we did geometry optimizations staring from the distorted structures by FPMD at 900 K and 1200 K and found that these two structures can easily recover to the initial configuration, indicative of high phase stability.

The aforementioned results can guarantee that CaSi monolayer is at least a good local minimum structure on the potential energy surface. Experimentally, the global minimum structures have more opportunities to be synthesized than the local minima. Is the ppSi-containing CaSi monolayer the global minimum? To address this issue, we performed a global structure search for CaSi in whole 2D space employing the particle-swarm optimization (PSO) method as implemented in CALYPSO code. As a benchmark, CALYPSO predicted the graphene and h-BN monolayer structures with two-atom hexagonal unit cells by only one generation, suggesting the reliability and efficiency of PSO algorithm in predicting stable 2D structures.

For 2D CaSi, we obtained three low-energy isomers within 30 generations, which are labeled as CaSi-I, CaSi-II, and CaSi-III (Fig. S5, ESI†). Actually, CaSi-I is just the ppSi-containing CaSi monolayer as discussed above. The structure of CaSi-II can be

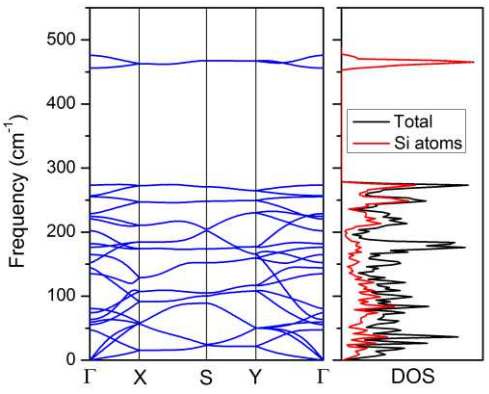

Fig. 3 Phonon spectrum (left) and phonon density of states (right) of CaSi monolayer computed using PBE functional.

described as Si tetramers embedded in distorted Ca octagons. Interestingly, all the Si atoms in CaSi-II are also quasi ppSi. In contrast to CaSi-I and CaSi-II, each Si atom in CaSi-III binds with four neighboring Ca atoms to form a ptSi moiety. According to DFT computations, CaSi-I is 86 and 392 meV/atom lower in energy than CaSi-II and CaSi-III, respectively. Therefore, our designed CaSi monolayer is actually the global minimum structure in 2D space, which is the first global minimum of ppSi-containing species. We propose that CaSi monolayer may be grown on suitable substrates by chemical vapor deposition (CVD) or molecular beam epitaxy (MBE) method, similar to growing silicene[50] and germanene[51] on metal or metal oxide surfaces.

Electronic and optical properties

After proving that CaSi monolayer is a stable structure with fantastic bonding frameworks, we are rather curious if this 2D sheet possesses some intriguing properties. To this end, we firstly computed the band structure and density of states (DOS) of CaSi monolayer to assess its electronic properties. As shown in Fig. 4a, an indirect band gap of 0.50 eV (0.07 eV by PBE functional, which tends to underestimate the band gap, Fig. S6, ESI†) appears in the band structure of CaSi monolayer. The valance band maximum (VBM) and conduction band minimum (CBM) are located at G (0, 0, 0) point and S (0.5, 0.5, 0) point, respectively. Therefore, different from silicene and other theoretically predicted Si-containing 2D structures (e. g. SiC_2,[35] Cu_2Si,[36] SiB_x,[55] $SiTi_x$[56]) which are semimetallic or metallic, CaSi monolayer is semiconducting with a considerable band gap. Noteworthy, the direct band gap lies in Y-G path (0.82 eV) is quite close to the indirect one. Note that the band gaps of most experimentally realized 2D semiconductors, such as BN,[57] MoS_2,[58] and phosphorene,[59] are all higher than 1.50 eV, whereas the 2D structures with a band gap in the range 0.3~1.5 eV are highly desirable in semiconductor industry.[60] Since CaSi monolayer has a rather suitable band gap, once synthesized it would find many important applications in electronics and optoelectronics. More interestingly, if all the atoms of CaSi monolayer were forced into the same plane, the band gap (0.77 eV, Fig. S7, ESI†) persists, indicating the robust semiconducting property of CaSi monolayer.

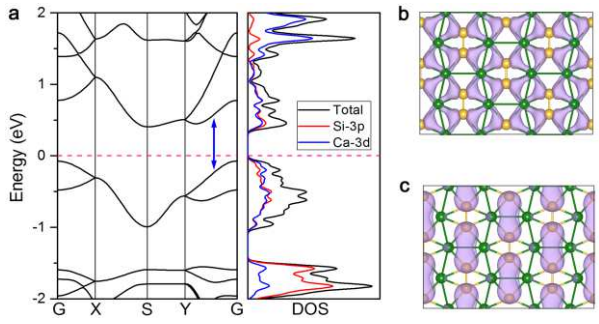

Fig. 4 (a) Band structure and density of states (DOS) of CaSi computed using HSE06 functional. The Fermi level is assigned at zero. The blue double-headed arrow denotes the direct band gap. Partial charge densities for the VBM (b) and CBM (c) of CaSi monolayer.

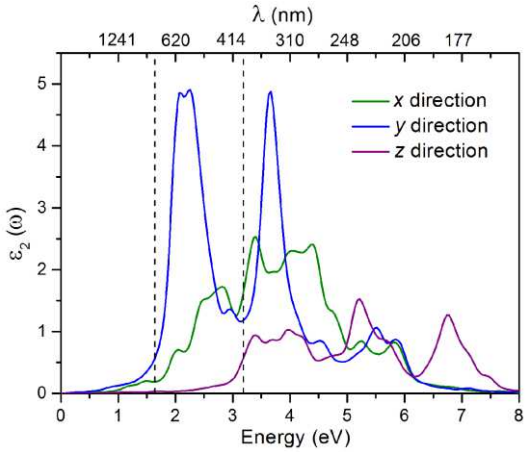

Fig. 5 Imaginary dielectric functions of CaSi monolayer along the *x*, *y* and *z* directions computed using HSE06 functional. The black dashed lines divide the light spectrum into infrared, visible, and ultraviolet regions (from left to right).

The partial DOS analysis demonstrates that the electronic states near the Fermi level of CaSi monolayer are mainly contributed by the Si-3p and Ca-3d orbitals. It manifests that the empty Ca-3d orbitals split in CaSi monolayer, and there is a finite probability for Si to back donate some of its received electrons to the low-lying 3d orbitals of Ca, leading to a partial occupancy of 3d orbitals as well as strong p-d hybridization. This electron donation/back-donation mechanism essentially helps stabilize the 2D CaSi network. We also plotted the partial charge densities associated with the VBM and CBM of CaSi monolayer to give a more explicit picture of its electronic structure. As shown in Fig. 4b and c, the VBM and CBM of CaSi monolayer are mainly contributed by the multicenter bonding and anti-bonding between Si and Ca atoms, respectively.

The moderate band gap would render CaSi monolayer a suitable candidate for optoelectronics. To give an intuitive demonstration of the optical properties, we also computed the imaginary part of the dielectric function (ε_2)[61] of CaSi monolayer using HSE06 functional (the PBE results are shown in Fig. S8, ESI†). As shown in Fig. 5, the optical absorption of CaSi monolayer along the *x* and *y* directions covers both visible and ultraviolet light regions. Remarkably, the absorption along the *y* the direction is much stronger than that of the x direction. In comparison to the *x* and *y* directions, the optical absorption along the *z* direction is much less pronounced.. The above results indicate that CaSi monolayer possesses good capacity for light-harvesting and has a unique optical anisotropy.

Mechanical properties

We also assessed the mechanical properties of CaSi monolayer by computing its elastic constants (C_{ij}). In accordance with the Born criteria,[62] a mechanically stable 2D structure should satisfy $C_{11}C_{22} - C_{12}^2 > 0$ as well as $C_{66} > 0$. For the small external

strains ε near the equilibrium positions, the elastic energy U_ε can be expressed as:

$$U_\varepsilon = E_\varepsilon - E_0 = \tfrac{1}{2}C_{11}\varepsilon_x^2 + \tfrac{1}{2}C_{22}\varepsilon_y^2 + C_{12}\varepsilon_x\varepsilon_y + 2C_{66}\varepsilon_{xy}^2 \quad (1)$$

where E_ε and E_0 are the total energies of strained and equilibrium structures, respectively. By fitting the energy curves associated with strains, the elastic constants were derived to be C_{11} = 22.37 N/m, C_{22} = 25.22 N/m, C_{12} = C_{21} = −3.68 N/m, and C_{66} = 10.51 N/m, which meet the aforementioned mechanical stability criteria, indicating that CaSi monolayer is mechanically stable.

On the basis of derived elastic constants, the in-plane Young's modules (Y) of CaSi monolayer can be computed by $Y_x = (C_{11}C_{22} - C_{12}C_{21})/C_{22}$ = 21.83 N/m and $Y_y = (C_{11}C_{22} - C_{12}C_{21})/C_{11}$ = 24.61 N/m, which are much lower than those of graphene (~341 N/m)[63] and MoS_2 monolayer (~128 N/m),[64] suggesting that CaSi monolayer is a rather soft material with good flexibility. The small difference in Young's modules in different directions indicates that CaSi monolayer is mechanically anisotropic to a rather small extent.

Remarkably, the negative C_{12} of CaSi monolayer leads to a negative Poisson's ratio of −0.15 (C_{21}/C_{22}) and −0.16 (C_{12}/C_{11}) in x and y directions, respectively. Physically, the Poisson's ratio is defined as the negative ratio of transverse contraction to the longitudinal extension. In nature most common materials have a positive Poisson's ratio as they will become thinner in cross section when they are stretched. Materials with a negative Poisson's ratio, which are known as auxetic materials,[65] can expand laterally when stretched. As a verification, we found that the equilibrium lattice constants of CaSi monolayer in the y(x) directions is stretched by ~0.3% when the lattice is subjected to a tensile strain of 2% in the x(y) direction (Fig. 6), confirming the negative Poisson's ratio of CaSi monolayer.

The negative Poisson's ratio would endow CaSi monolayer with multiple merits, such as enhanced toughness, self-adaptive vibrational damping and improved shear stiffness. With so fascinating mechanical properties, CaSi monolayer can be utilized in many specific fields, e. g. superior dampers, pizeocomposites, and nanoauxetic materials. Recently, 2D black phosphorus has been first predicted theoretically[66] and then observed experimentally[67] to have a Poisson's ratio. Some hypothetical 2D nanostructures, including but not limited to penta-graphene,[68] borophane,[69] silica[70] and our previously designed Be_5C_2 monolayer[33] were also revealed to possess a Poisson's ratio. Note that the negative Poisson's ratio of black phosphorus and borophane were observed in the out-of-plane direction, while the negative Poisson's ration of our CaSi monolayer was found in the in-plane direction. Remarkably, the negative Poisson's ratio of CaSi monolayer is much higher than those of black phosphorus, penta-graphene and borophane, and is comparable to those of silica and Be_5C_2 monolayer. No doubt, the unusual negative Poisson's ratio in these 2D structures should be derived from the novel atomic configurations.

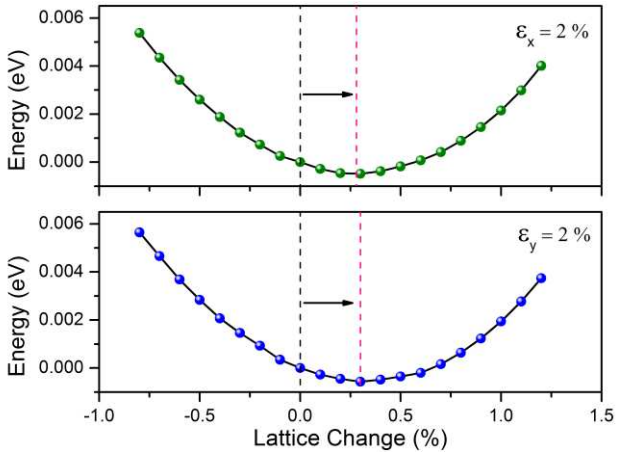

Fig. 6 Relative energy as the function of the lattice change on y (a) and x (b) direction when CaSi monolayer is subjected to a 2% tensile strain along the x and y direction, respectively. The initial and equilibrium magnitudes of lattice constant changes are highlighted as black and red dashed lines, respectively.

Conclusions

To summarize, inspired by the bonding pattern of $Ca_4Si_2^{2-}$, a local minimum containing a ppSi center, we designed a new 2D material, namely CaSi monolayer, by means of comprehensive DFT computations. In CaSi monolayer, each Si atom binds with four Ca atoms and one neighboring Si atoms in almost the same plane, forming a quasi ppSi moiety. CaSi monolayer has rather high thermodynamic, kinetic and thermal stabilities, and is the lowest-energy structure on the 2D energy potential surface. The fundamental mechanism of stabilizing ppSi in CaSi monolayer is due to the electron donation/back-donation between Si and Ca atoms. Superior to semimetallic silicene, CaSi monolayer is semiconducting with an indirect band gap of 0.5 eV. It has rather strong optical absorption in the visible as well as infrared regions of solar spectrum. Especially, CaSi monolayer exhibits a rather unusual negative Poisson's ratio. With the development of experimental techniques for fabrication of 2D materials, we believe that CaSi monolayer can be achieved in laboratory in the near future, and its excellent properties and potential applications can be explored. Our work once again highlights the structure-property relationship of materials, and we hope that our work could stimulate more theoretical and experimental efforts on designing new materials with rule-breaking chemical bonding.

Acknowledgements

Support in China by Natural Science Foundation of China (No. 21522305 and 21403115), the NSF of Jiangsu Province of China (No. BK20150045) and Innovation Project in Jiangsu Province (KYZZ16_0454), and in USA by National Science Foundation (Grant EPS-1010094) and Department of Defense (Grant W911NF-12-1-0083) is gratefully acknowledged. The computational resources utilized in this research were provided by Shanghai Supercomputer Center.

References

1 J. H. van't Hoff, *Arch. Neerl. Sci. Exactes Nat.*, 1874, 445.
2 J. A. LeBel, *Bull. Soc. Chim. Fr.*, 1874, **22**, 337.
3 H. J. Monkhorst, *Chem. Commun.*, 1968, 1111.
4 R. Hoffmann, R. W. Alder and C. F. Wilcox, *J. Am. Chem. Soc.*, 1970, **92**, 4992.
5 J. B. Collins, J. D. Dill, E. D. Jemmis, Y. Apeloig, P. v. R. Schleyer, R. Seeger and J. A. Pople, *J. Am. Chem. Soc.*, 1976, **98**, 5419.
6 F. A. Cotton and M. Millar, *J. Am. Chem. Soc.*, 1977, **99**, 7886.
7 P. v. R. Schleyer and A. I. Boldyrev, *J. Chem. Soc. Chem. Commun.*, 1991, 1536
8 A. I. Boldyrev and J. Simons, *J. Am. Chem. Soc.*, 1998, **120**, 7967.
9 W. Siebert and A. Gunale, *Chem. Soc. Rev.*, 1999, **28**, 367.
10 G. Merion, M. A. Mendez-Rojas, A. Vela and T. Heine, *J. Comput. Chem.*, 2007, **28**, 362.
11 L. -M. Yang, E. Ganz, Z. Chen, Z. -X. Wang and P. v. R. Schleyer, *Angew. Chem. Int. Ed.*, 2015, **54**, 9468.
12 X. Li, L.-S. Wang, A. I. Boldyrev and J. Simons, *J. Am. Chem. Soc.*, 1999, **121**, 6033.
13 X. Li, H. F. Zhang, L. S. Wang, G. D. Geske and A. I. Boldyrev, *Angew. Chem., Int. Ed.*, 2000, **39**, 3630.
14 L. S. Wang, A. I. Boldyrev, X. Li and J. Simons, *J. Am. Chem. Soc.*, 2000, **122**, 7681.
15 Z. X. Wang and P. v. R. Schleyer, *Science*, 2001, **292**, 2465.
16 Y. Pei, W. An, K. Ito, P. v. R. Schleyer and X. C. Zeng, *J. Am. Chem. Soc.*, 2008, **130**, 10394.
17 K. Exner and P. v. R. Schleyer, *Science*, 2000, **290**, 1937.
18 K. Ito, Z. F. Chen, C. Corminboeuf, C. S. Wannere, X. H. Zhang, Q. S. Li and P. v. R. Schleyer, *J. Am. Chem. Soc.*, 2007, **129**, 1510.
19 M. B. Krogh-Jesperson, J. Chanderasekhar, E. –U. Würthwein, J. B. Collins and P. v. R. Schleyer, *J. Am. Chem. Soc.*, 1980, **102**, 2263.
20 E. –U. Würthwein and P. v. R. Schleyer, *Angew. Chem. Int. Ed.,* 1979, **18**, 553.
21 A. I. Boldyrev, P. v. R. Schleyer and R. Keese, *Mendeleev Commun.*, 1992, **2**, 93.
22 P. Belanzoni, G. Giorgi, G. F. Cerofolini and A. Sgamellotti, *J. Phys. Chem. A*, 2006, **110**, 4582.
23 A. I. Boldyrev, X. Li and L. S. Wang, *Angew. Chem. Int. Ed.*, 2000, **39**, 3307.
24 S. D. Li, C. –Q. Miao, J. –C. Guo and G. –M. Ren, *J. Am. Chem. Soc.,* 2004, **126**, 16227.
25 R. Islas, T. Heine, K. Ito, P. v. R. Schleyer and G. Merino, *J. Am. Chem. Soc.*, 2007, **129**, 14767.
26 P. D. Pancharatna, M. A. Mendez-Rojas, G. Merino, A. Vela and R. Hoffmann, J. Am. Chem. Soc., 2004, 126, 15309.
27 L. M. Yang, Y. H. Ding and C. C. Sun, *J. Am. Chem. Soc.*, 2007, **129**, 658.
28 M. H. Wu, Y. Pei and X. C. Zeng, *J. Am. Chem. Soc.*, 2010, **132**, 5554-5555.
29 X. J. Wu, Y. Pei and X. C. Zeng, *Nano Lett.*, 2009, **9**, 1577.
30 Z. Zhang, X. Liu, B. I. Yakobson and W. Guo, *J. Am. Chem. Soc.*, 2014, **133**, 19326.
31 Y. Li, Y. Liao, P. v. R. Schleyer and Z. Chen, *Nanoscale*, 2014, **6**, 10784.
32 J. Dai, X. Wu, J. Yang and X. C. Zeng, *J. Phys. Chem. Lett.*, 2014, **5**, 2058.
33 Y. Wang, F. Li, Y. Li and Z. Chen, *Nat. Commun.,* 2016, **7**, 11488.
34 Y. Li, Y. Liao and Z. Chen, *Angew. Chem. Int. Ed.*, 2014, **53**, 7248.
35 Y. Li, F. Li, Z. Zhou and Z. Chen, *J. Am. Chem. Soc.,* 2011, **133**, 900.
36 L. -M. Yang, V. Bačić, I. A. Popov, A. I. Boldyrev, T. Heine, T. Frauenheim and E. Ganz, *J. Am. Chem. Soc.*, 2015, **137**, 2757.
37 B. Feng, B. Fu, S. Kasamatsu, S. Ito, P. Cheng, C. Liu, Y. Feng, S. Wu, S. K. Mahatha, P. Sheverdyaeva, P. Moras, M. Aritam O. Sugino, T. Chiang, K. Shimada, K. Miyamoto, T. Okuda, K. Wu, L. Chen. Y. Yao and I. Matsuda, *Nat. Commun.,* 2016, **8**, 1007.
38 Y. Zhao and D. G. Truhlar, *Theor.Chem. Acc.,* 2008, **120**, 215.
39 M. J. Frisch, et al. *GAUSSIAN 03*, Revision E.02, Gaussian, Inc., Wallingford, CT, 2004, see the ESI† for the full reference.
40 J. A. Pople, M. Head-Gordon and K. Raghavachari, *J. Chem. Phys.*, 1987, **87**, 5968
41 G. Kresse and J. Hafner, *Phys. Rev. B*, 1993, **47**, 558.
42 J. P. Perdew, L. Burke and M. Ernzerhof, *Phys. Rev. Lett.*, 1996, **77**, 3865.
43 P. E. Blöchl, *Phys. Rev. B*, 1994, **50**, 17953.
44 G. Kresse and D. Joubert, *Phys. Rev. B*, 1999, **59**, 1758.
45 J. Heyd, G. E. Scuseria and M. Ernzerhof, J. Chem. Phys., 2006, **124**, 219906.
46 A. Togo, F. Oba and I. Tanaka, *Phys. Rev. B*, 2008, **78**, 134106.
47 T. R. Galeev, B. D. Dunnington, J. R. Schmidt and A. I. Boldyrev, *Phys. Chem. Chem. Phys.*, 2013, **15**, 5022.
48 G. J. Martyna, M. L. Klein and M. E. Tuckerman, *J. Chem. Phys.*, 1992, **97**, 2635.
49 Y. Wang, J. Lv, L. Zhu and Y. Ma, *Phys. Rev. B*, 2010, **82**, 094116.
50 P. Vogt, P. D. Padava, C. Quaresima, J. Avila, E. Frantzeskakis, M. C. Asensio, A. Resta, B. Ealet and G. L. Lay, *Phys. Rev. Lett.*, 2012, **108**, 155501.
51 L. Li, S. Lu, J. Pan, Z. Qin, Y. Wang, Y. Wang, G. Cao, S. Du and H. Gao, *Adv. Mater.*, 2014, **25**, 4820.
52 F. Zhu, W. Chen, Y. Xu, C. Gao, D. Guan, C. Liu, D. Qian, S. –C. Zhang, J. Jia. *Nat. Mater.*, 2015, **14**, 1020.
53 A. Molina-Sánchez and L. Wirtz, *Phys. Rev. B*, 2011, **84**, 155413.
54 S. Cahangirov, M. Topsakal, E. Akturk, H. Sahin, S. Ciraci, *Phys. Rev. Lett.*, 2009, **102**, 236804.
55 J. Dai, Y. Zhao, X. Wu, J. Yang and X. Zeng, *J. Phys. Chem. Lett.*, 2013, **4**, 561.
56 Q. Wu, J. –J. Zhang, P. Hao, Z. Ji, S. Dong, C. Ling, Q. Chen and J. Wang, *J. Phys. Chem. Lett.*, 2016, **7**, 3723.
57 A. Nag, K. Raidongia, K. P. S. S. Hembram, R. Datta, U. V. Waghmare and C. N. R. Rao, *ACS Nano*, 2010, **4**, 1539.
58 K. F. Mak, C. Lee, J. Hone, J. Shan and T. F. Heinz, *Phys. Rev. Lett.*, 2010, **105**, 136805.
59 L. Li, Y. Yu, G. J. Ye, Q. Ge, X. Ou, H. Wu, D. Feng, X. H. Chen, Y. Zhang, *Nat. Nanotech.,* 2014, **9**, 372.
60 L. Li, J. Kim, C. Jin, G. J. Ye, D. Y. Qiu, F. H. Da Jornada, Z. Shi, L. Chen, Z. Zhang, F. Yang, K. Watanabe, T. Taniguchi, W. Ren, S. G. Louie, X. H. Chen, Y. Zhang and F. Wang, *Nat. Nanotech.,* 2017, **12**, 21.
61 M. Gajdoš, K. Hummer and G. Kresse, *Phys. Rev. B*, 2006, **73**, 045112.
62 M. Born and H. Huang, Dynamical theory of crystal lattices, Clarendon, Oxford, 1954.
63 Q. Peng, X. Wen and S. De, *RSC Adv.*, 2013, **3**, 13772.
64 Y. Cai, G. Zhang and Y. –W. Zhang, *J. Am. Chem. Soc.*, 2014, **136**, 6269-6275.
65 R. S. Lakes, *Science*, 1987, **235**, 1038.
66 J. W. Jiang and H. S. Park, *Nat. Commun.*, 2014, **5**, 4727.
67 Y. Du, J. Maassen, W. Wu, Z. Luo, X. Xu and P. D. Ye, *Nano Lett.*, 2016, **16**, 6701.
68 S. Zhang, J. Zhou, Q. Wang, X. Chen, Y. Kawazoe and P. Jena, *Proc Natl Acad Sci USA*, 2015, **112**, 2372.
69 L. Kou, Y. Ma, C. Tang, Z. Sun, A. Du and C. Chen, *Nano Lett.*, 2016, **16**, 7910.
70 V. O. Özçelik, S. Cahangirov and S. Ciraci, *Phys. Rev. Lett.*, 2014, **112**, 246803.